Anal. Chem. **2010,** *82,* 3780–3787

Propagating Surface Plasmon Resonance on Microhole Arrays

Ludovic S. Live,[†] Olivier R. Bolduc,[†] and Jean-François Masson*[,†,‡,§]

Département de Chimie, Centre for Self-Assembled Chemical Structures (CSACS), and Centre for Biorecognition and Biosensors (CBB), Université de Montréal, C. P. 6128 Succ. Centre-Ville, Montréal, Qc, Canada H3C 3J7

Metallic thin films patterned with micrometer size triangle or hole arrays present plasmonic properties when excited in the Kretschmann configuration, that are improved in comparison to conventional thin film surface plasmon resonance (SPR). These optical properties can be tuned by varying the physical aspects of the microplasmonic structures. Triangles and microhole arrays were prepared with modified nanosphere lithography (NSL) using latex spheres of 0.65, 0.82, 1.0, 1.5, or 3.2 μm in diameter. This allowed the preparation of triangles with edge lengths between 275 to 2000 nm and microhole arrays of various periodicities, diameters, and hole depths. These microstructures were studied to understand the relationship between the physical aspects and the optical properties, such as the sensitivity, working refractive index range, spectral width of the plasmonic peaks, spectral noise, and refractive index resolution. Microhole arrays with a hole diameter equal to half the periodicity were found to combine the advantages of both localized surface plasmon resonance (LSPR) on nanoparticles and SPR on a thin film. These microhole arrays exhibited high sensitivity to refractive index (>3000 nm/RIU), sensitivity to monolayer formation (2-fold improvement compared to thin films), and excellent refractive index resolution (10^{-6} RIU). Finally, a biosensor for the detection of 10 nM of immunoglobulin G (IgG) exhibited a greater response with microplasmonic materials compared to conventional thin Au films. Hence, these novel plasmonic materials exhibit a strong potential as an SPR sensing platform. They can be implemented on existing instrumentation and use detection protocols developed for current SPR sensors.

Surface plasmon resonance is a powerful analytical technique for label-free detection with high sensitivity of biomolecules based on the optical properties of plasmonic materials.[1,2] SPR instruments typically use thin continuous metallic films, usually with Au or Ag as the plasmonic materials. These metals present a sharp and intense plasmonic band in their total internal reflectance spectrum when excited in the Kretschmann configuration of SPR.[1,2] While the position of the plasmonic peak corresponds to a specific refractive index at the metal/dielectric interface, real-time monitoring of its position gives kinetic information of binding processes occurring at the SPR sensor surface. In sensing experiments, molecular interactions occur in close proximity to the metal surface, creating a small, albeit measurable, change of refractive index (RI). As a result, SPR is very sensitive to the binding of biomolecules to the Au or Ag surface. Although this configuration of SPR has been very useful to monitor binding interactions of biomolecules in the nanomolar to picomolar range, sensitivity improvement remains important to detect biomolecules in the femtomolar to picomolar range. SPR sensor performance could be improved by developing novel plasmonic materials with greater sensitivity and shorter penetration depth.

Among possibilities to improve the sensing performance of SPR-based sensors, the optical properties can be tuned by changing the size, shape, and composition of the metal particle or film.[3] By tuning the optical properties of plasmonic materials, other parameters such as the spectral aspect of the SPR band and the RI linearity range have to be considered, as they also affect the quality of a SPR sensor. Also of consideration, novel plasmonic materials should be based on simple fabrication methodologies and require little or no changes to existing instrumentation. One approach that was developed with success consists of tuning the sensing volume of SPR. Of particular interest, localized surface plasmon resonance (LSPR) has a short penetration depth of the electric field, which increases the SPR response measured upon binding events.[4] Hence, LSPR is widely employed with nanoparticles,[5−7] nanohole arrays,[8,9] nanorings,[10] nanorods,[11] nanocrescents,[12] and nanoshells.[13] Although LSPR is

* To whom correspondence should be addressed. Tel: 1-514-343-7342. Fax: 1-514-343-7586. E-mail: jf.masson@umontreal.ca.

[†] Département de Chimie.

[‡] Centre for Self-Assembled Chemical Structures.

[§] Centre for Biorecognition and Biosensors.

(1) Homola, J. *Anal. Bioanal. Chem.* **2003**, *377*, 528–539.

(2) Homola, J.; Yee, S. S.; Gauglitz, G. *Sens. Actuators, B* **1999**, *54*, 3–15.

(3) El-Sayed, M. A. *Acc. Chem. Res.* **2004**, *37*, 326–333.

(4) Malinsky, M. D.; Kelly, K. L.; Schatz, G. C.; Van Duyne, R. P. *J. Am. Chem. Soc.* **2001**, *123*, 1471–1482.

(5) Jensen, T. R.; Malinsky, M. D.; Haynes, C. L.; Van Duyne, R. P. *J. Phys. Chem. B* **2000**, *104*, 10549–10556.

(6) Link, S.; El-Sayed, M. A. *Int. Rev. Phys. Chem.* **2000**, *19*, 409–453.

(7) Jain, P. K.; Huang, X. H.; El-Sayed, I. H.; El-Sayed, M. A. *Acc. Chem. Res.* **2008**, *41*, 1578–1586.

(8) Coe, J. V.; Heer, J. M.; Teeters-Kennedy, S.; Tian, H.; Rodriguez, K. R. *Annu. Rev. Phys. Chem.* **2008**, *59*, 179–202.

(9) Gordon, R.; Sinton, D.; Kavanagh, K. L.; Brolo, A. G. *Acc. Chem. Res.* **2008**, *41*, 1049–1057.

(10) Kim, S.; Jung, J. M.; Choi, D. G.; Jung, H. T.; Yang, S. M. *Langmuir* **2006**, *22*, 7109–7112.

(11) Huang, X. H.; El-Sayed, I. H.; Qian, W.; El-Sayed, M. A. *J. Am. Chem. Soc.* **2006**, *128*, 2115–2120.

(12) Bukasov, R.; Shumaker-Parry, J. S. *Nano Lett.* **2007**, *7*, 1113–1118.

(13) Wu, D. J.; Xu, X. D.; Liu, X. J. *J. Chem. Phys.* **2008**, *129*, 074711.

10.1021/ac100177j
Published on Web 03/31/2010

advantageous due to the short penetration depth and large response to binding events, it is currently limited by low bulk RI sensitivity and RI resolution.

Alternatively, most investigations to improve SPR on a Kretschmann configuration have been aimed at increasing the sensitivity to the refractive index of thin continuous films by using Ag/Au bilayers,[14] an indium tin oxide thin overlayer,[15] and nanoparticles over metallic film.[16] Significant improvement of the optical properties was observed with long-range surface plasmon resonance (LRSPR) for a Teflon layer positioned between the prism and the metallic film on a Kretschmann configuration SPR.[17] A sensitivity 8 times greater than that of conventional SPR and a refractive index resolution as low as 10^{-8} RIU were observed with this novel plasmonic propagation mode.[18] However, the long penetration depth of LRSPR makes it more suitable for large molecule sensing such as for virus and bacteria.[18] Another approach of interest uses nanorods orientated normally to a metallic film. These nanorod films were active in LSPR and SPR with a high sensitivity of 3×10^4 nm/RIU and a probing depth of 500 nm.[19] Otherwise, improved sensitivity was achieved for nanopatterned films with periodic nanowires,[20] nanogrooves,[21] and isolated nanoparticle films.[22] These approaches are especially interesting, as multiple techniques have been designed to pattern surfaces in the recent years. However, the novel plasmonic materials mainly involve continuous or nanostructured thin films.

To date, very few studies report the plasmonic properties of micrometer size plasmonic structures. This contrasts with the large amount of research undertaken on LSPR with nanoparticles and SPR with macroscopic thin films. However, it is known that micrometer size Au films support a surface plasmon. It was previously reported that SPR was excited on a metalized tip apex of a scanning near-field optical microscope.[23] Based on this principle, refractive index sensors were built with a microscopic thin metallic film at the tip of an etched fiber.[24,25] The sensing region of these etched fibers were on the order of a few micrometers. Although the etched fibers exhibited sensitivity to refractive index, the noise level was high, resulting in poor RI resolution. The complexity associated with these measurements makes it difficult to fully investigate the properties of microstructures using this technique. Hence, a method based on nanosphere lithography (NSL) was recently developed to investigate the optical properties of micrometer size Au triangles, with an SPR instrument in the Kretschmann configuration.[26,27] Fabricating triangle arrays with nanospheres of different sizes tunes the area of the micrometer size Au films. These micrometer size triangle arrays proved to be active in both LSPR (measured in transmission spectroscopy) and SPR (measured on a Kretschmann configuration SPR). The refractive index sensitivity of these triangle arrays was measured to be up to 2000 nm/RIU from the SPR-active peak. Also, a penetration depth of 24 nm was calculated for microtriangles,[26] which is comparable to the probing distance observed in LSPR.[4]

Applying NSL to fabricate microplasmonic structures provides a simple tool to tailor the physical aspects of the Au microstructures and study the optical properties on a Kretschmann configuration SPR. Recently, NSL was modified to fabricate nanohole arrays.[28−35] This modified technique involves etching the NSL mask with an oxygen plasma. The nanospheres are etched to a smaller diameter, while maintaining the position of the sphere in the crystalline lattice. Depositing a metal film on this NSL mask and removing it creates a nanohole array. Depending on the orientation of the lattice, nanohole arrays have a long continuous Au film between rows of holes, while other orientations have short island-like films of Au.[27] This technique is also suitable to fabricate microhole arrays. It is important to map the plasmonic properties of microstructured films to assess the potential of these materials as sensing platforms. Hence, micropatterned thin films with triangle and microhole arrays must be investigated with different periodicities, hole diameters, and depths (film thickness). The structure-dependent sensitivity to RI, penetration depth, spectral noise, and RI resolution using Kretschmann configuration SPR will establish the potential of microplasmonic structures for SPR biosensors.

EXPERIMENTAL SECTION

Preparation of the Microplasmonic Materials and Continuous Films. The continuous thin films were prepared by coating directly a clean glass coverslip with a 2 nm Ti adhesion layer and a 50 nm Au film. Au triangle and microhole arrays were fabricated according to a modified NSL method published elsewhere.[26,27,34] Herein, the latex sphere masks were drop coated on a clean glass coverslip. A 10% solution of the latex spheres with diameters of 0.65, 0.82, 1.0, 1.5, and 3.2 μm was mixed with ethanol and water (Table 1). Volumes between 35 and 40 μL of the solution mixture were drop coated on each clean 22×22 mm

(14) Zynio, S. A.; Samoylov, A. V.; Surovtseva, E. R.; Mirsky, V. M.; Shirshov, Y. M. *Sensors* **2002**, *2*, 62–70.
(15) Szunerits, S.; Castel, X.; Boukherroub, R. *J. Phys. Chem. C* **2008**, *112*, 15813–15817.
(16) Hutter, E.; Fendler, J. H.; Roy, D. *J. Phys. Chem. B* **2001**, *105*, 11159–11168.
(17) Nenninger, G. G.; Tobiska, P.; Homola, J.; Yee, S. S. *Sens. Actuators, B* **2001**, *74*, 145–151.
(18) Vala, M.; Etheridge, S.; Roach, J. A.; Homola, J. *Sens. Actuators, B* **2009**, *139*, 59–63.
(19) Kabashin, A. V.; Evans, P.; Pastkovsky, S.; Hendren, W.; Wurtz, G. A.; Atkinson, R.; Pollard, R.; Podolskiy, V. A.; Zayats, A. V. *Nat. Mater.* **2009**, *8*, 867–871.
(20) Byun, K. M.; Yoon, S. J.; Kim, D.; Kim, S. J. *Opt. Lett.* **2007**, *32*, 1902–1904.
(21) Malic, L.; Cui, B.; Tabrizian, M.; Veres, T. *Opt. Expr.* **2009**, *17*, 20386–20392.
(22) Wark, A. W.; Lee, H. J.; Qavi, A. J.; Corn, R. M. *Anal. Chem.* **2007**, *79*, 6697–6701.
(23) Devaux, E.; Dereux, A.; Bourillot, E.; Weeber, J. C.; Lacroute, Y.; Goudonnet, J. P.; Girard, C. *Phys. Rev. B* **2000**, *62*, 10504–10514.
(24) Abrahamyan, I.; Nerkararyan, K. *Phys. Lett. A* **2007**, *364*, 494–496.
(25) Kurihara, K.; Ohkawa, H.; Iwasaki, Y.; Niwa, O.; Tobita, T.; Suzuki, K. *Anal. Chim. Acta* **2004**, *523*, 165–170.
(26) Live, L. S.; Masson, J. F. *J. Phys. Chem. C* **2009**, *113*, 10052–10060.
(27) Live, L. S.; Murray-Methot, M. P.; Masson, J. F. *J. Phys. Chem. C* **2009**, *113*, 40–44.
(28) Canpean, V.; Astilean, S. *Mater. Lett.* **2009**, *63*, 2520–2522.
(29) Canpean, V.; Astilean, S. *Nucl. Instrum. Methods Phys. Res., Sect. B:* **2009**, *267*, 397–399.
(30) Cong, C. X.; Junus, W. C.; Shen, Z. X.; Yu, T. *Nanoscale Res. Lett.* **2009**, *4*, 1324–1328.
(31) Huang, W. H.; Sun, C. H.; Min, W. L.; Jiang, P.; Jiang, B. *J. Phys. Chem. C* **2008**, *112*, 17586–17591.
(32) Lee, S. H.; Bantz, K. C.; Lindquist, N. C.; Oh, S. H.; Haynes, C. L. *Langmuir* **2009**, *25*, 13685–13693.
(33) Murray, W. A.; Astilean, S.; Barnes, W. L. *Phys. Rev. B* **2004**, *69*, 165407.
(34) Murray-Methot, M. P.; Menegazzo, N.; Masson, J. F. *Analyst* **2008**, *133*, 1714–1721.
(35) Sun, C. H.; Min, W. L.; Jiang, P. *Chem. Commun.* **2008**, 3163–3165.

Table 1. Mixture of Latex Spheres, Ethanol, and Water Used To Prepare Sphere Masks by Drop Coating[a]

diameter (μm)	spheres (v%)	ethanol (v%)	water (v%)
3.2	20	20	60
1.5	15	15	70
1.0	13	27	60
0.82	20	30	50
0.65	12	16	72

[a] Volumes between 35 and 40 μL of mixture solution are used to prepare a mask.

glass slide and dried slowly over a few hours using a Petri dish cover to decrease the evaporation rate. This preparation method results in a well-ordered monolayer with large areas over 10 mm^2 for 1.0, 1.5, and 3.2 μm spheres. Latex spheres of 0.82 and 0.65 μm produced a well-ordered monolayer over slightly smaller areas. For the metalization step, a 2 nm thick adhesive layer of Ti was deposited on the sample prior to the Au deposition. At this stage, if Au was deposited over this NSL mask, a pattern of metal triangle arrays remained on the glass slide following removal of the mask. The sphere masks were slightly etched prior to metalization, which allows the preparation of 50 nm thick triangles with 3.2, 1.5, and 1.0 μm sphere masks corresponding to triangle edge lengths of 2.0, 1.0, and 0.75 μm, respectively. This process was also applied to fabricate nanotriangles with 0.82 and 0.65 μm spheres, which result in triangle edge lengths of 475 and 275 nm with thicknesses of 40 and 25 nm, respectively.

Otherwise, microhole arrays were prepared by etching the sphere mask with reactive ion etching (RIE) in an oxygen plasma chamber (Harrick PG-32). The oxygen flow was set at 15−20 mL/min in the plasma chamber, which was operated at 16 W. Four samples were etched simultaneously in the chamber with an average etch rate around 60 nm/min using these settings. Therefore, the etch time (between 2 and 75 min) controls the size of the spheres, while the periodicity of the microhole array is the initial diameter of the sphere mask. The microhole arrays prepared with this method had a small standard deviation of 70 nm on the diameter of the holes. Once Au is deposited, the spheres were removed with ultrasound using a mixed water/ethanol solution, and the microhole arrays remained on the glass slide. A series of microhole arrays with 0.65, 0.82, 1.0, 1.5, and 3.2 μm periodicities and a broad range of diameters were prepared with RIE using oxygen plasma.

Physical and Optical Characterization of Microstructured Films. The physical properties of triangle and microhole arrays were systematically measured by atomic force microscopy (AFM) in contact mode (Figure 1). Areas of 5 × 5 to 40 × 40 μm^2 (depending on the initial sphere diameter) were scanned to obtain the topographic image of the samples. The structure edge length and height for triangles or diameter and depth for microhole arrays were obtained with the cross-section analysis of the AFM image. For triangle and microhole arrays of 1.0, 1.5, and 3.2 μm periodicity, the thickness of the metal film deposited was set at 50 nm, unless otherwise indicated. For triangles of 0.82 and 0.65 μm periodicities, the thickness of Au was limited to ~40 nm. The SPR measurements were performed with a home-built SPR instrument in the Kretschmann configuration based on a dove prism.[36] The SPR response was probed from a sample area < 10 mm^2. The SPR signal was monitored in the wavelength range between 400 and 900 nm with a spectrophotometer based on a 150 g/mm grating blazed at 500 nm. Each spectrum was an average of 200 acquisitions with an integration time of 20 ms/acquisition. The processed SPR spectrum was obtained in Matlab software as a ratio of the P and S polarization of light. The wavelength position of the SPR active band was calculated using a minimum-finding algorithm.

Monolayer Formation. A monolayer of 16-mercaptohexadecanoic acid (16-MHA) was formed on the Au microstructures with a 5 mM solution of 16-MHA in dimethylformamide (DMF). Samples were immersed in this solution overnight and then washed thoroughly with ethanol. The SPR response was measured in water before and after the formation of a monolayer. The difference in SPR wavelength was used to calculate the SPR response due to monolayer formation.

SPR Biosensors. The glass slide with the microhole arrays, the triangle arrays, or the continuous film was immersed in a 1 mM solution of 3-MPA-(histidine)$_3$-(aspartic acid)$_2$-OH synthesized on hydroxymethyl polystyrene resin (EMD Biochemicals, Ville Mont-Royal, QC) where 3-MPA stands for 3-mercaptopropionic acid (Sigma-Aldrich, Milwaukee, WI). After 16 h in the 3-MPA-(histidine)$_3$-(aspartic acid)$_2$-OH solution, the samples were washed with ethanol and dried. Then, the modified Au surfaces were placed on a wavelength interrogation SPR instrument equipped with a 100-μL fluidic cell for kinetic measurements.[36] Prior to the acquisition of the S polarized spectrum, the fluidic chamber was filled with 18 MΩ water for a stabilization period of 5 min. Thereafter, the P polarized light was used for real-time monitoring of each reaction performed on the SPR sensor. After 2 min in water, an aqueous solution composed of 100 mM *N*-ethyl-*N*′-(3-dimethylaminopropyl)carbodiimide (EDC, Fluka) and 20 mM of *N*-hydroxysuccinimide (NHS, Sigma-Aldrich) was injected for 2 min followed by a rinsing step with phosphate buffered saline (PBS, pH 4.5) for 2 min.[37,38] Immobilization of the antibody was accomplished from the reaction of 25 μg/mL antihuman IgG (Cedarlane Laboratories Ltd., Burlington, ON) with the EDC/NHS activated surface for 15 min. The anti-IgG solution was prepared in PBS at pH 7.4. PBS was injected for 2 min to rinse unbound antibody. The next step required the injection of 1 M ethanolamine solution adjusted to pH 8.5 for 5 min. This step deactivated the unreacted NHS sites on the monolayer. PBS was injected on the SPR sensor once again to result in the IgG-specific biosensor. The SPR detection of 10 nM immunoglobulin G (IgG) solution in PBS was performed for 5 min. Reversibility of IgG binding was monitored in PBS for 5 min. IgG detection was measured at least three times with each plasmonic material.

RESULTS AND DISCUSSION

The potential of microstructured Au films in Kretschmann-based SPR was assessed by a thorough investigation of the optical

(36) Bolduc, O. R.; Live, L. S.; Masson, J. F. *Talanta* **2009**, *77*, 1680–1687.
(37) Johnsson, B.; Löfås, S.; Lindquist, G.; Edström, Å.; Hillgren, R.-M. M.; Hansson, A. *J. Mol. Recogit.* **1995**, *8*, 125–131.
(38) Löfås, S.; Johnsson, B.; Tegendal, K.; Rönnberg, I. *Colloids Surf., B* **1993**, *1*, 83–89.

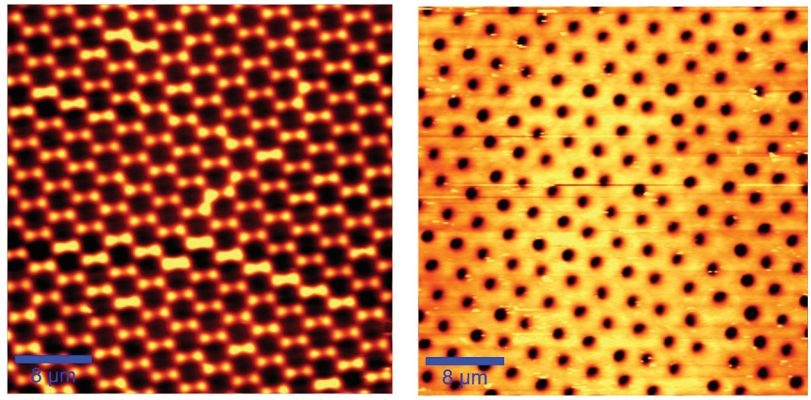

Figure 1. AFM images of micropatterned thin films with microtriangle (left) and microhole arrays (right) prepared with 3.2 μm spheres.

and analytical properties of these plasmonic materials. In order to be useful, these structures should improve current analytical properties of continuous Au thin films. Moreover, the micropatterned Au films should exhibit optical properties within the same wavelength/angle range. This would allow their use on existing SPR instruments. Therefore, the plasmonic properties were investigated with Au microhole arrays for various periodicities (spacing between holes), diameters, and depths of the microhole. Each of the different physical parameters was varied independently of the others. In a first experiment, micropatterned Au thin films of 50 ± 10 nm thickness were prepared with a modified NSL technique using latex spheres of 0.65, 0.82, 1.0, 1.5, and 3.2 μm in diameter. The initial diameter of the spheres is equal to the periodicity. Second, triangle and microhole arrays were fabricated with different hole diameters for every period. In order to compare microhole arrays of different periodicities on the same basis, a diam/period scale was established. From this scale, three regimes were observed: triangles (diam/period > 0.7), microhole arrays (0 < diam/period < 0.7), and continuous films (diam/period = 0). Moreover, Au microstructures of fixed periodicity and diam/period were investigated for thicknesses varying from 20 to 200 nm (see Supporting Information). In this work, each of the investigated parameters is an average of at least three (n = 3) samples. Thereby, a complete map of the structure-dependent plasmonic properties was established.

Sensitivity to Refractive Index. The sensitivity to refractive index of the SPR active band is often used as a comparative point for different plasmonic structures. Here, the sensitivity to bulk refractive index was measured in Kretschmann configuration SPR for continuous films, triangles, and microhole arrays with aqueous sucrose solutions between 1.33 to 1.39 RIU. The sensitivity of continuous films is well characterized and will serve as a reference point. Because of the nonlinearity of SPR in the 1.33 to 1.39 RIU range, the sensitivity for the whole range is taken into account in this work. For continuous Au films, a linear calibration model within the 1.33 to 1.39 RIU range results in sensitivity of 2742 nm/RIU. However, the sensitivity calculated from the tangent of a polynomial fit for Au films is 1765 nm/RIU at 1.33 RIU, which increases to 2248 nm/RIU at 1.36 RIU and 3870 nm/RIU at 1.38 RIU. The sensitivity of the microstructures will therefore be compared to these values.

The SPR spectrum for triangles is characterized by two transmission minima of low sensitivity and one transmission maximum of higher sensitivity.[26,27] The transmission maximum is the only peak considered herein, as it is the only one with a measurable sensitivity. Triangle arrays 50 nm thick presented a SPR active transmission maximum band with sensitivity ranging from 1065 nm/RIU in 2000 nm triangles to 770 nm/RIU in 475 nm triangles (Table 2). It was noted that the sensitivity slightly decreases with smaller periodicity. In every case, the sensitivity of the microtriangles is lower than that for continuous films. However, this is not the case for microhole arrays. First, the SPR spectrum of microhole arrays is very similar to SPR on a continuous film. A strong absorption peak is observed near λ = 600 nm with microhole arrays, also characteristic of propagating SPR on continuous films. This plasmonic band exhibits sensitivity to refractive index, as observed from the redshift of the SPR active band with increasing refractive index (Figure 2, left panel). The sensitivity for every microhole array is equal or greater than for a continuous film (Table 3). The sensitivity is between 4200 and 2800 nm/RIU for each microhole array investigated here. A significant increase in sensitivity was observed for microhole arrays with 0.65 μm periodicity and for the 1.5 and 3.2 μm microhole arrays near a diam/period of 0.6.

Table 2. Sensitivity to Refractive Index between 1.33 and 1.39 RIU of the Transmission Maximum Band with Au Triangles

periodicity (μm)	edge length (nm)	height (nm)	$\delta\lambda/\delta\eta$ (nm/RIU)
3.2	2000	49	1065
1.5	1000	46	849
1.0	750	47	796
0.82	475	37	770
0.65	275	25	869

Width of the SPR Band in Microstructures. The quality of the sensing performance with plasmonic materials is not only a function of sensitivity but also of the precision at which the SPR wavelength can be measured. Generally, the precision of the SPR wavelength is closely related to the spectral aspect of the SPR active band. Specifically, the full-width at half-maximum (fwhm) and the intensity of the SPR band gives a good estimate of the precision for SPR bands. A sharp and intense band is required to improve resolution of spectroscopic techniques. In the case of microstructures, the SPR active band is either a transmission maximum for triangle or an absorption peak for microhole arrays and continuous thin films. The methodology to calculate the intensity and fwhm is demonstrated in Figure 3 (top left). Since SPR is an asymmetrical spectroscopic peak, the intensity was

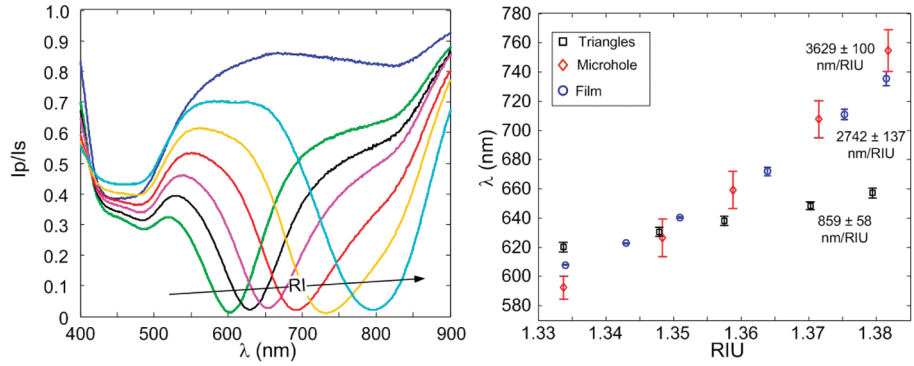

Figure 2. (Left) SPR calibration spectra of microhole arrays measured in air (RI = 1.0, dark blue) and sucrose solution of RI = 1.3337 (green), 1.3484 (black), 1.3588 (violet), 1.3715 (red), 1.3817 (yellow), 1.3942 (light blue). (Right) Calibration curves of SPR sensors with sucrose solutions. The calibration curve represents the average response from three independent samples.

Table 3. Sensitivity to Refractive Index in nm/RIU for Au Microhole Arrays with Different Diam/Period (*D*/*P*)[a]

3.2 μm		1.5 μm		1.0 μm		0.82 μm		0.65 μm	
D/P	$\delta\lambda/\delta\eta$	D/P	$\delta\lambda/\delta\eta$	D/P	$\delta\lambda/\delta\eta$	D/P	$\delta\lambda/\delta\eta$	D/P	$\delta\lambda/\delta\eta$
0.58	4238	0.57	4244	0.60	3681	0.43	2929	0.39	4217
0.48	3325	0.43	3046	0.47	3357	0.35	3398	0.26	4145
0.28	3253	0.36	2924	0.29	2826	0.22	3091		
0.14	3281	0.30	2744	0.25	3050				

[a] The sensitivity for continuous films is 2742 nm/RIU.

measured from the baseline with the lowest intensity drop. Thus, the fwhm was measured at the halfway intensity point from this way of measuring the intensity. This provides a good estimate of both parameters.

The intensity and the fwhm of the SPR band are dependent on the physical aspect of the structures. The transition from the SPR signal obtained in triangles to the SPR signal in continuous Au films is clearly observed for microstructures with a periodicity of 3.2 μm (Figure 3, top right). The SPR response of intermediate diam/period exhibits spectral features characteristic of triangles and continuous films. Initially, the SPR active band in water for triangles is a broad transmission maximum around $\lambda = 625$ nm. This SPR band transitions to an absorption minimum in microhole arrays (diam/period < 0.7). The SPR band in microhole arrays sharpens and is more intense with decreasing diam/period (as the microhole arrays increasingly resemble a continuous film). The periodicity also affects the SPR response in microhole arrays. The SPR response, with a diam/period of approximately 0.3, is sharper and more intense for 3.2 μm periodicity, which broadens and weakens as the periodicity decreases (Figure 3, bottom left). Also, microhole arrays of 3.2 μm periodicity exhibit a SPR response spectroscopically similar to continuous films.

In order to compare with a single parameter the variations of intensity and fwhm, the characterization of the SPR active band will be performed based on the fwhm ratio, which is the fwhm divided by intensity of the SPR band. This intensity is measured as the intensity reflected divided by the initial intensity, ranging from 0 for a complete absorption of light to 1 for 100% transmission. A small fwhm ratio indicates a sharp and/or intense SPR response while a higher fwhm ratio characterizes a weak and/or broad SPR response (Figure 3, bottom right). Continuous films presented the lowest fwhm ratio at approximately 100. For microhole arrays of diam/period < 0.5, the fwhm ratio is relatively constant between 100 and 200, similar to continuous films. This indicates that the periodicity slightly impacts the fwhm ratio for the smaller diam/period, which exhibits the lowest fwhm ratio. However, for microhole arrays of diam/period > 0.5, the fwhm ratio increases rapidly to nearly 1000 for diam/period of 0.7. Triangles also exhibit an fwhm ratio greater than 500. The optimal sensing platform should combine both high refractive index sensitivity and resolution. Therefore, the structures with optimal sensitivity and fwhm ratio are microhole arrays with diam/period between 0.5 and 0.1.

Penetration Depth (l_d). In biosensing, a shorter l_d increases the SPR response of the sensing platform for binding events occurring close to the Au surface. Therefore, a short l_d is highly advantageous in a biosensor format where the measurement principle is based on surface binding events. The penetration depth is a measure of the distance that the SPR electric field probes into the surrounding medium. For continuous films, l_d is usually between 200 and 500 nm,[2] but under our experimental conditions, the l_d is roughly 230 nm. However, the penetration depth is much smaller at around 20 nm with nanoparticles LSPR.[4] The penetration depth for triangle and microhole arrays was experimentally measured with the SPR response to the formation of a monolayer of 16-mercaptohexadecanoic acid (16-MHA). The excitation wavelength of the SPR band was measured in water before and after the formation of a monolayer. The difference in the SPR response gives the SPR shift ($\Delta\lambda$) due to the formation of a monolayer.

The lowest response to formation of a monolayer was obtained with the continuous Au films. The SPR shift initially increases with larger diam/period and plateaus for microstructures of larger diam/period (Figure 4, left). Triangles and hole arrays with a diam/period > 0.5 present the highest SPR response $\Delta\lambda = 12$ nm, which is over 2 times greater than the SPR response with continuous films ($\Delta\lambda = 5.5$ nm). The penetration depth can be obtained experimentally from the SPR response of the monolayer formation. The calculations were performed based on the equations introduced by Jung et al.[39] The calculated l_d showed a linear decrease of the penetration depth with increasing diam/period. Thus, a continuous film exhibits a l_d of 230 nm, and microplasmonic structures have a tunable l_d between 250 and 30 nm

(39) Jung, L. S.; Campbell, C. T.; Chinowsky, T. M.; Mar, M. N.; Yee, S. S. *Langmuir* **1998**, *14*, 5636–5648.

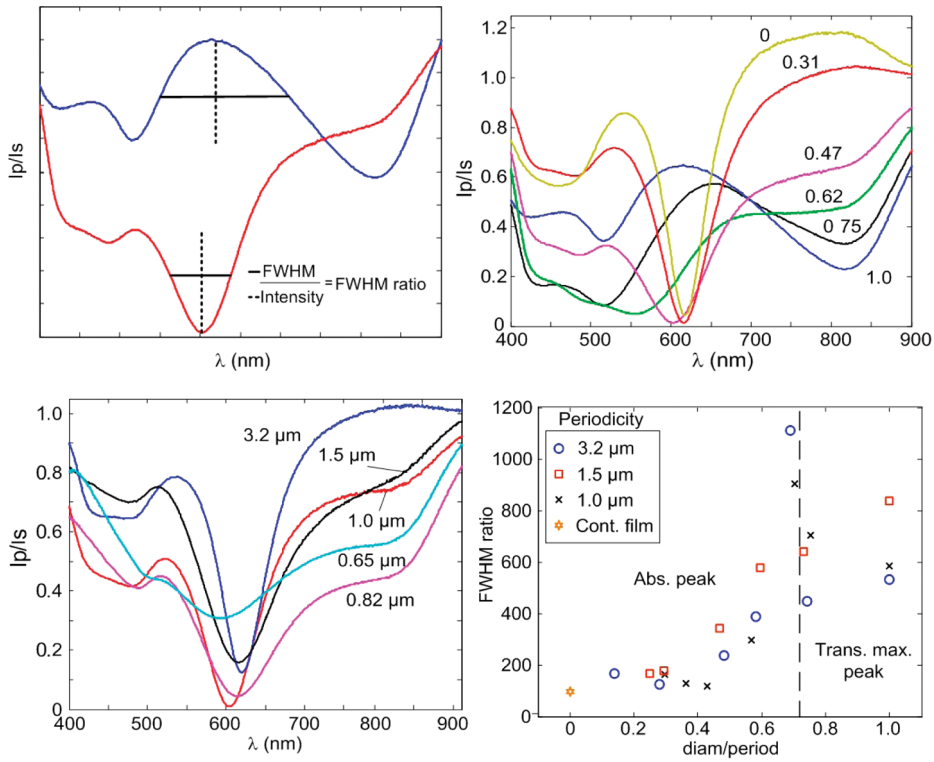

Figure 3. (Top left) Methodology to calculate the fwhm ratio for triangles (blue curve) and for microhole arrays (red curve). (Top right) The SPR spectra for water were measured with microhole arrays of 3.2 μm periodicity with diam/period between 0 and 1. (Bottom left) SPR response in water for microhole arrays near 0.3 diam/period with various periodicities. (Bottom right) The fwhm ratio decreases for smaller diam/period. This value must be minimized for optical analytical performance.

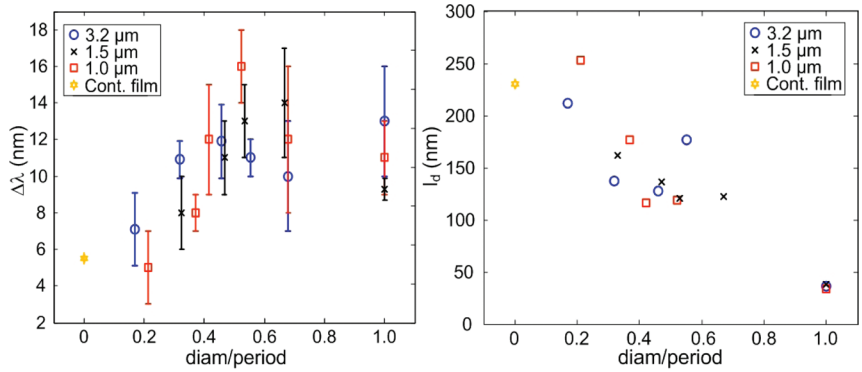

Figure 4. (Left) Wavelength shift of the SPR absorption band measured in water solution from the formation of a 16-MHA monolayer and (right) the calculated penetration depth from this shift.

(Figure 4, right). Triangles and microhole arrays present a penetration depth shorter than for continuous films. This shorter penetration depth is advantageous, as it results in a larger SPR response from binding events. Therefore, microhole arrays have a great potential as a sensing platform because of its high refractive index sensitivity, excellent fwhm ratio, and improved response to binding events. Hence, the following sensing experiments were performed with 3.2 μm microhole arrays with diam/period = 0.5.

Sensing Performances with Microhole Arrays. In this section, the sensing performances of 3.2 μm microhole arrays with diam/period of 0.5 are compared with triangles of 1.8 μm edge length and continuous thin films which are currently used as a SPR sensing platform. Analytical parameters such as the spectral noise and the refractive index resolution were investigated in kinetic experiments. The SPR signal was measured as a function of time in water and phosphate buffer solution (PBS) (ΔRI < 0.002). Water and PBS was successively injected on the SPR sensors made with the different plasmonic materials (Figure 5). The sensorgram measured with triangles and continuous films presents a similar SPR response of $\Delta\lambda = 1.8$ nm while microhole arrays exhibit a greater shift at $\Delta\lambda = 2.7$ nm (Table 4). The spectral noise was calculated as the standard deviation of 100 data points for the SPR measurement in PBS. The spectral noise for the sensorgram with triangle arrays (0.096 nm) is worse by 1 order of magnitude than continuous films and microhole arrays (0.0027 and 0.0055 nm, respectively). The slightly larger noise with microhole arrays compared to continuous films can be explained by the somewhat larger fwhm ratio observed with microhole arrays. The RI resolution was determined from the spectral noise

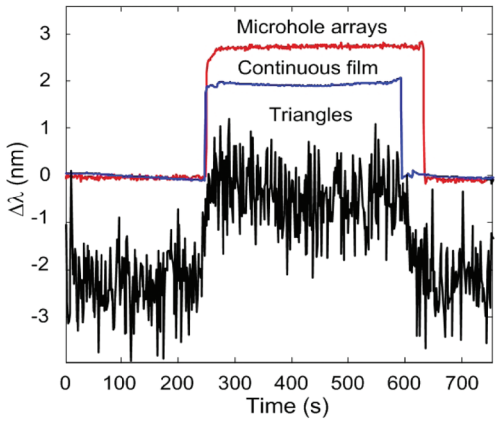

Figure 5. Sensorgrams for SPR sensors with different plasmonic materials. A short exposure of the sensor to water (1.33400 RIU) is followed by addition of a phosphate buffer solution (PBS, 1.33566 RIU). The SPR response of triangles (dark lines) is offset for ease of representation.

Table 4. Analytical Parameters of Triangles, Microhole Arrays, and Continuous Films in Kinetic Measurements

	$\Delta\lambda$ (nm)	spectral noise (nm)	resolution (RIU)
continuous films	1.8 ± 0.3	0.0027	1.5×10^{-6}
microhole arrays	2.7 ± 0.4	0.0055	1.5×10^{-6}
triangles	1.8 ± 0.4	0.096	1.1×10^{-4}

divided by the sensitivity to refractive index. The resolution with microhole arrays and continuous thin films is 1.5×10^{-6} RIU, while the resolution with triangle arrays is limited to 10^{-4} RIU. The significantly worse RI resolution of triangle arrays is caused by the lower sensitivity and the larger fwhm ratio. It is important to note that the resolution was obtained without data preprocessing, which could improve the RI resolution by nearly 1 order of magnitude.[36] Thus, microhole arrays and continuous films are comparable platforms in terms of resolution and spectral noise. However, microhole arrays showed improved SPR response under other experimental conditions, as described in the sections above.

IgG Biosensors with Different Plasmonic Materials. The potential of using plasmonic microstructures as a biosensing platform was investigated with the detection of 10 nM IgG. In this experiment, the SPR response to IgG was measured with microhole arrays, triangle arrays of 1.8 μm edge length, and continuous films. The surface of each plasmonic material was functionalized with anti-IgG, resulting in a specific response to IgG. The SPR response with triangles within the first 300 s is much greater than for the microhole arrays and for the Au thin film (Figure 6). The SPR response to 10 nM IgG was the largest for the triangle arrays at 2.1 ± 0.6 nm, significantly larger than for microhole arrays (0.91 ± 0.18 nm) and for continuous films (0.69 ± 0.11 nm). A significantly larger error on the IgG shift was observed for triangle arrays due to the relatively large width of the plasmonic band, decreasing the precision of the peak position measurement. As noted above, the RI resolution is significantly worse for triangle arrays. The increase in the SPR response to IgG with microstructures compared to thin Au films is likely to be due to the shorter penetration depth for these materials. Continuous films have the longest penetration depth of these

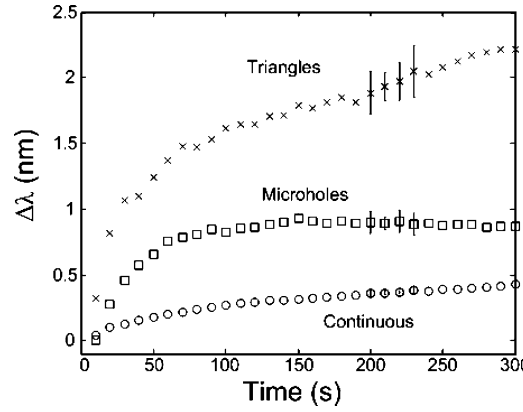

Figure 6. Sensogram for the detection of 10 nM IgG with different plasmonic materials: triangles (×), microhole arrays (□), and continuous films (○). The error bars represent two standard deviations on the data points.

plasmonic materials, which results in the smallest response to the IgG binding event. Microhole arrays have a shorter penetration depth than the continuous films, thus a larger SPR response. Lastly, IgG binding to the triangle arrays exhibited the shortest penetration depth among the plasmonic materials tested and has the largest response to IgG binding. A shorter penetration depth generally results in a greater SPR response to binding events occurring close to the sensing surface. This demonstrates that microplasmonic materials are advantageous for biosensing.

It is also noteworthy to point out the different aspects of the binding curves from IgG on the various plasmonic substrates. Of particular interest, thin films have the longest response time to IgG binding, while microhole and triangle arrays rapidly reach a plateau for SPR response. This difference in SPR response for monolayer formation and for IgG binding may be explained by the number of immobilized receptors per unit area on each surface. The triangles should have the fewest number of receptors per unit area, as the surface is mainly covered by glass with Au triangular islands. As the surface transitions from Au triangle arrays to microhole arrays to thin films, the area covered by Au increases and thus should the number of receptors per unit area. On the length scale of the microstructures, IgG diffuses rapidly (on the order of hundreds of micrometers during the 300 s detection time). Thus, for identical IgG concentration (as in this experiment), IgG will reach equilibrium more rapidly as the number of IgG molecules required to reach equilibrium is smaller with the same number of IgG molecules available. To support this, we have observed a similar phenomenon with 16-MHA monolayer formation. Triangle arrays reach a SPR response of 13 nm within 1 h,[26] which corresponds to a full monolayer (Figure 4, left). In the case of thin Au films, the SPR response was at 2 nm within 1 h,[26] which increased to 5.5 nm for a full monolayer (Figure 4, left). It also demonstrates a faster reaction/response time with monolayer formation using microstructured films.

CONCLUSIONS

Metallic thin films with triangle or microhole arrays are active in SPR when excited in Kretschmann configuration SPR. These microplasmonic materials exhibited structure-dependent plasmonic properties which improve the sensing performance of SPR compared to continuous Au films. The sensitivity to refractive

index and the sensitivity to monolayer formation or binding events were improved with microhole arrays. Otherwise, the refractive index resolution, the fwhm ratio, and the spectral noise were all equivalent or similar to those of continuous Au films. The optimal microstructure was found to be microhole arrays of diam/period = 0.5. Other advantages of these microplasmonic materials include the ease of fabrication and the use of current SPR instrumentation without modifications. To demonstrate the biosensing potential of these materials, an IgG biosensor was constructed on triangle and microhole arrays using standard chemical derivations of the surface. The SPR response for a 10 nM IgG solution was improved significantly with triangle and microhole arrays compared to the response obtained with continuous thin films. Therefore, these structures could replace currently used continuous Au films, with minimal modifications to protocols.

ACKNOWLEDGMENT

Financial support was provided by NanoQuébec, the Canadian Space Agency, the Canada Foundation for Innovation (CFI), the National Sciences and Engineering Research Council of Canada (NSERC), the Fonds Québécois de la Recherche sur la Nature et les Technologies (FQRNT).

SUPPORTING INFORMATION AVAILABLE

The effect of Au film thickness on the SPR response. This information is available free of charge via the Internet at http://pubs.acs.org.

Received for review January 20, 2010. Accepted March 10, 2010.

AC100177J